

The Optimisation and Production of Stable Homogeneous Amine Enriched Surfaces with Characterised Nanotopographical Properties for Enhanced Osteoinduction of Mesenchymal Stem Cells

Rui Chen¹, John A. Hunt², Sandra Fawcett³, Raechelle D'Sa¹, Riaz Akhtar¹ and Judith M. Curran^{1*}

1. *Dr J.M. Curran, Dr Rui Chen, Dr Akhtar and Dr R. D'Sa, Centre for Materials and Structures, School of Engineering, Harrison Hughes Building, University of Liverpool, U.K. L69 3GH j.curran@liv.ac.uk
2. Professor J.A. Hunt, Medical Technologies and Advanced Materials, Nottingham Trent University, U.K. NG11 8NS
3. Dr S. Fawcett, Clinical Engineering, Institute of Ageing and Chronic Disease, University of Liverpool, U.K. L69 3GA

Keywords:

Osteoinduction, Nanotopography, Surface Chemistry, Surface Characterisation and Mesenchymal Stem Cells

This article has been accepted for publication and undergone full peer review but has not been through the copyediting, typesetting, pagination and proofreading process which may lead to differences between this version and the Version of Record. Please cite this article as an 'Accepted Article', doi: 10.1002/jbm.a.36383

Abstract

Silane modification has been proposed as a powerful biomaterial surface modification tool.

This is the first comprehensive investigation into effect of silane chain length on the resultant properties of $-NH_2$ silane monolayers (SAMS) and the associated osteoinductive properties of the surface. A range of $-NH_2$ presenting silanes, chain length 3 to 11, were introduced to glass coverslips and characterised using water contact angles, atomic force microscopy, X-ray photoelectron spectroscopy and Ninhydrin assays. The ability of the variation in chain length to form a homogenous layer across the entirety of the surfaces was also assessed. The osteoinductive potential of the resultant surfaces was evaluated by real time polymerase chain reaction, immunocytochemistry and von Kossa staining. Control of surface chemistry and topography was directly associated with changes in chain length. This resulted in the identification of a specific, chain length 11 (CL11) which significantly increased the osteoinductive properties of the modified materials. Only CL11 surfaces had a highly regular nano-topography/roughness which resulted in the formation of an appetite-like layer on the surface that induced a significantly enhanced osteoinductive response (increased expression of osteocalcin, CBFA1, sclerostin and the production of a calcified matrix) across the entirety of the surface.

Introduction

It is well proven that cells respond to stimuli at the sub-micron/nano scale⁽¹⁻⁴⁾. To investigate and exploit this and realise the potential of material induced cell responses, material design and surface modification must be considered at the sub-micron scale, so that we can establish base line material data that can be used to inform future biomaterial design and produce materials that efficiently induce biological responses in the absence of exogenous biological stimuli. The development and optimisation of technologies that can translate into a manufacturing process to meet these design criteria is essential if the potential of biomaterials in regenerative medicines is to be achieved⁽⁵⁾. Silane modification offers a way to enrich a surface with a specific chemical group and is a process that can be applied to an array of base substrates, therefore it is a process that offers significant potential in biomaterials research, especially in inducing osteogenesis in mesenchymal stem cells⁽⁶⁻⁸⁾. To fulfil its potential as a cost effective surface modification tool, the resultant SAMs layer must have the ability to produce a homogenous cellular response across the entirety of the area of interest.

The rationale behind the need for bottom-up control of cell responses is derived from controlling cell function via directing interactions with a surface rather than taking this as benign or inevitable constant. Material induced control of biological responses encompasses research into the effect of surface chemistry⁽⁹⁻¹¹⁾, topography⁽¹²⁾ and stiffness^(13, 14) on cellular responses. All of these approaches show potential, but fundamental systematic knowledge regarding the optimal combination of material properties required to initiate effective control over cell function is still lacking.

We, and others, have previously reported on the potential of silane modifications as a mechanism for enriching the surfaces of silicon, gold, glass, PLGA and PCL with $-CH_3$, $-NH_2$, $-OH$ and $-COOH$ and the resultant variable effect on stem cell adhesion and differentiation^(6, 7, 15-18). Within these studies the effect of varying the chain length for a specific chemical moiety was not addressed, nor were the resulting surfaces considered at the sub-micron scale. To summarise the results from these studies $-NH_2$ modifications demonstrated an osteoinductive potential and $-OH$ and $-COOH$ substrates were chondrogenic. Whilst these results were reproducible on all base substrates tested the response was heterogeneous across the entire surface of test substrates, this resulted in clusters of differentiating cells in separate areas and heterogeneous cell populations. The lack of optimisation of the observed cellular responses was attributed to the fact that the studies considered and characterised the generic properties of the silane modified surface i.e. tested to see if a chemical group had been introduced and the resultant effect of surface energy/hydrophobicity.

The need for the optimisation of silane modification protocols was further enhanced as other studies have demonstrated that cells can sense and respond to stimuli at the sub-micron scale and the emerging role of nanotopography in osteoinduction of stem cells^(15, 16, 19). In addition recent studies have also proven that combinations of chemistry and nanotopography can be used to enhance material induced control of cell adhesion and subsequently cell function on model surfaces⁽²⁰⁾. Appropriate control of this phenomenon, at a single cell level can lead to material induced enhanced control of cell phenotype via selected integrin adhesion, focal contact formation and subsequent mechanotransduction events^(18, 21, 22).

We have previously reported on the potential of silane modified surfaces as a mechanism for enriching the surface with $-CH_3$ and their role in stem cell isolation/expansion⁽²³⁾. In addition to chemically enriching a surface, silane modifications can be used to induce reproducible changes in nanotopographical profiles, via changes in the chain length (CL) associated with the silane. This combination of factors i.e. chemistry and topography has resulted in a material induced control of protein binding, subsequent integrin adhesion and the production of a superior MSC population (significantly increased expression of MSC markers across the entirety of the surface). Therefore detailed systematic research using silane modified substrates as a technique for providing sub-micron control of chemical group deposition and associated topography, on a range of clinically relevant materials is an essential step in developing the next generation of cost effective interactive (smart) biomaterials. This approach can readily be applied to understanding and optimising the parameters associated with $-NH_2$ self-assembled monolayers (SAMS) and the associated potential in osteoinduction of a MSC population.

This paper reports on the design, production and characterisation of an amine ($-NH_2$) presenting cost effective coating technology that utilises silane modification technologies and examines the effect of chain length of the silane as a mechanism for controlling the surface properties of the resultant modified monolayer across the entirety of the substrate. The research determines the optimal combination of sub-micron material modification properties that produced a highly osteoinductive surface for human adult mesenchymal stem cells (hMSC) on glass surfaces. The optimised coating resulted in the production of a mature osteoblast phenotype from a well characterised mesenchymal stem cell population. The potential biomimetic properties of these surfaces are also investigated, via their ability

to directly adsorb calcium and phosphate from solutions, producing osteoinductive matrices in which the cells become embedded.

The data presented within this paper is relevant and significant for both in vitro and in vivo manipulation of human mesenchymal stem cells (hMSCs). The research presented within this article focuses on modified glass substrates that have a role in in vitro investigations, whilst data presented in the supplementary figures highlights the translational aspect of the work by presenting data associated with validating the ability of specific silane chain lengths to enhance the osteoinductive nature of modified PLGA.

Glass coverslips were silane modified, using a range of chain lengths associated with the –NH₂ presenting silane. The range of surfaces were characterised at a number of random locations across the entirety of the surface using XPS, Ninhydrin, Static Water Contact Angle (WCA) and Atomic Force Microscopy (AFM) to ensure reproducibility and evaluate homogeneity of chemical group deposition and associated nanotopographical profiles across the entirety of the surface. The well-defined test substrates were evaluated for their ability to induce osteogenic differentiation of MSCs, in basal medium, and data was characterised to fully assess the combinatorial effect of homogenous –NH₂ surface enrichment and controlled nanotopography on the osteoinductive potential.

Experimental Section

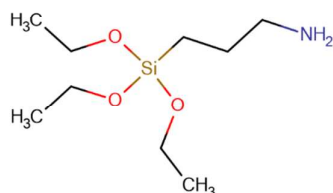
Material production and modification

Glass preparation and modification

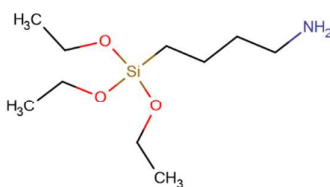
Materials preparation

13mm glass coverslips were cleaned using a 0.5M solution of sodium hydroxide (Sigma, UK) for 30 minutes in an ultrasonic bath, followed by washing in 3 changes of distilled water, then placed in 1M Nitric acid for 30 minutes in an ultrasonic bath. Samples were washed again with 3 changes of distilled water and dried in a 50°C oven. Clean coverslips were then modified using the following 0.1M silanes for 30 minutes. CL3 (3-Aminopropyl) triethoxysilane (Sigma), CL4 4-(triethoxysilyl) butan-1-amine (Fluorochem), and CL11 11-Aminoundecyltriethoxysilane (Fluorochem). Samples were then washed with Isopropyl alcohol for 5 minutes 3 times and then washed with distilled water. Concentrations of silanes were based upon preliminary experiments that have tested a range of concentrations 0.05M to 0.25M and reaction times from 30 seconds to 2 hours, the conditions utilised in this study provided the most homogenous covering per chain length and allowed a direct comparison between different chain lengths associated with the $-NH_2$ presenting silane (data not shown).

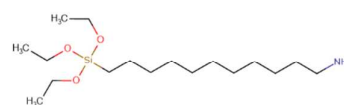
Molecular Structures of CL3, CL4 and CL11;



CL3



CL4



CL11

Contact angle measurement

Static contact angles of the samples in deionised water were analysed using the Sessile Drop method at room temperature by Theta Lite Optical Tensiometer (TL100, Attension, Biolin Scientific, Finland). To determine the contact angle, the shapes of the water droplet on the solid surface were automatically recorded and the resultant images were analysed by built-in software One-Attension. A total of 4 samples of each type of material for control and modified surfaces were analysed. For each sample three different points were measured at random points across the surface to check surface uniformity. Values are shown as mean +/- standard deviation. Statistical analysis was carried out using one way ANOVA (Tukey analysis), $p=0.05$.

Ninhydrin Assay

The distribution of the $-NH_2$ groups on the silane modified surfaces were qualitatively evaluated using a Ninhydrin assay. 0.35g of Ninhydrin (Fluka, UK) was dissolved in 100ml of ethanol. 1ml of this solution was placed on each of the samples and incubated for 5 minutes at $90^\circ C$. The solution was removed from the coverslips. The modified coverslips were photographed showing a qualitative colour change on the surface of the substrate and the homogenous distribution of $-NH_2$ groups across the entirety of the surface, magnifications appropriate to image the entirety of 1 coverslip in the field of view were used. A total of 4 repeats were carried out to qualitatively assess the reproducibility of the formation of $-NH_2$ enriched areas on a surface, representative images are shown.

X-Ray Photoelectron Spectroscopy (XPS)

X-ray photoelectron spectroscopy (XPS) was carried out using a Kratos Axis Ultra DLD spectrometer (Kratos, Telford, UK) using a monochromated AlK α x-ray (1486.6eV) source operating at a power of 150W (voltage: 15 kV, current: 10 mA). All spectra were recorded using a “slot” aperture and spectra were recorded below 5×10^{-8} Torr on three spots on each sample. A magnetic immersion lens was used to charge neutralise the samples. Binding energy (BE) positions were further charge corrected by calibrating the C-C/C-H component to 285.0 eV. A pass energy of 160 eV and 20 eV were used to record the wide energy survey spectra (1-1300 eV) and the high resolution spectra respectively. The relative atomic % concentration (at. %), was calculated using CasaXPS version 2.3.15 software (Casa software, UK). Spectra were curve fitted after the linear background subtraction using a mixed Gaussian-Lorentzian (70:30) function. A total of four repeats per sample were analysed. Data are reported as average values \pm 1 standard deviation.

Atomic Force Microscopy (AFM) of modified glass coverslips

AFM imaging was carried out using a commercial AFM (NanoScope VIII MultiMode AFM, Bruker Co., Santa Barbara, CA, USA) equipped with 150 x 150 x 5 μ m scanner (J-scanner). The ScanAsyst mode was applied using silicon probe (Bruker RTESPA-150A, nominal frequency of 150 kHz, nominal spring constant of 5N/m) with a scan resolution of 256 samples per line at a scan rate of 0.6Hz. 3 images of 1.4 μ m x 1.4 μ m were obtained for each sample. In total, 3 separate samples per chain length were imaged at random points across the surface, representative micrographs are shown. All post-image analysis was carried out using Bruker NanoScope Analysis software v1.5. Root mean square (R_q) was determined using the Particle Analysis feature within the software.

Phosphorous adsorption/ Elemental Analysis and von-Kossa

The ability of the modified substrates to adsorb calcium and phosphate ions from Phosphate Buffered Saline solution was evaluated both qualitatively (von Kossa) and quantitatively (Elemental Analysis). The silane modified samples were inserted into a 24 well plate, along with an untreated glass control and incubated at 37°C, 5%CO₂ for 7 days with either dH₂O (control) or 25%, 50% or 100% Phosphate Buffered Silane containing calcium and magnesium (Sigma UK). 100% PBS solution was made up according to the manufacturers guide lines (100% equates to a standard PBS solution that is recommended by the manufacturer and proven to be optimal for as a reagent to support tissue culture) and serial dilutions were made by diluting the 100% PBS solution with the appropriate volume of dH₂O. The resulting samples were removed from the solution and left to dry at room temperature for 24 hours. The samples were then examined using X-ray analysis and stained using Von Kossa stain for mineralisation.

Von Kossa: Samples were hydrated using 3 submersions in distilled water for 2 minutes each, then covered with 2% silver nitrate solution (Sigma UK) and placed under a UV lamp for 1 hour. Samples were washed with dH₂O and placed in a 2.5% sodium thiosulphate solution (Sigma UK) for 3 minutes. Samples were then washed with dH₂O and counterstained using Harris's haematoxylin (Sigma UK) for 5 minutes, washed in running tap water for 5 minutes and differentiated in 1% acid alcohol for 2 seconds before being washed in distilled water. Samples were then dehydrated through increasing concentrations of alcohols (70%, 90% and 100%) for 2 minutes each and cleared in xylene (BDH, UK) for 2 minutes then mounted with glass coverslips in DPX (BDH, UK). Samples were visualised using Zeiss Apatome (Zeiss, Germany).

X-ray analysis: Elemental analysis of the samples immersed in contact with the PBS solutions was undertaken to evaluate levels of mineralisation on the surface. Baseline data was extrapolated from dry films (not cultured in contact with any solution) to ensure that minerals present were as a direct result of chemical interactions with the surface when then samples were exposed to PBS. Dried samples were prepared using a carbon coater (EMTECH, UK) and X-ray microanalysis was performed using a LEO 1550 SEM (Zeiss, UK) with an INCA system. 4 repeats were carried out and in each repeat points of analysis were generated at 5 distinct locations on the film, from these fields 10 spectra were generated at random. Statistical analysis was used to calculate the probability of phosphate ion adsorption occurring on the surface based on the raw data. This was calculated using the total number of spectra taken (50 per repeat), divided by the number of positive spectra (phosphate ion adsorption) found, representing the incidence of the presence of the phosphate ion on the test substrates. 0=no probability and 1= high probability.

Qualitative Evaluation of Protein Adsorption

The ability of the modified surfaces to adsorb fibronectin was qualitatively evaluated using immunofluorescent staining. Human fibronectin solutions (5 μ g/ml, Sigma) were prepared under sterile conditions and cultured in contact with the test samples. The concentration was optimised based on previous studies (data not included). Samples were incubated for 24 hours, and then removed from culture, washed with PBS and fixed using 4% Formaldehyde /2% Sucrose. Fibronectin adsorption was visualised by labelling with sheep anti-human fibronectin primary antibody 10 μ g/ml (Serotec) attached to Rhodamine conjugated goat IgG 10 μ g/ml (ICN). Full details of the staining protocol are provided below, samples were visualised using confocal microscopy, LSM510, Zeiss. For qualitative

evaluation of protein adsorption 3 repeats were carried out and 3 images were taken from each repeat, representative images are shown.

The change in the associated nanotopographical profile associated with the adsorbed protein layer was quantified using previously described methods (AFM experimental methods).

MSC culture

Characterised 4P hMSC (Lonza, UK) were cultured in contact with the test samples at a concentration of 5×10^4 ml and a volume of 1ml cell solution was seeded onto the substrates and cultured using basal MSC growth media (Lonza, UK) in 24 well plates at 37°C, 5%CO₂ for 14 and 28 days.

Real Time PCR Analysis

mRNA was isolated using the standard guanidinium isothiocyanate Tri Reagent™ (Sigma, UK) protocol, followed by treatment with deoxyribonuclease I (Invitrogen) prior to reverse transcription. Reverse transcription was carried out using previously described methods and optimized primers⁽²⁴⁾. Real Time PCR was carried out using SYBR Green (Biorad) mastermix supported by the iCycler system (Biorad). Standard 15µl reactions (2µl cDNA, 0.5µl of 100 µM sense primer, 0.5µl 100 mM anti-sense primers, 7.5µl SYBR Green mastermix (Biorad) and 4.5µl RNase free water) were carried out in triplicate. A total of four repeats per sample were carried out and all data was normalised to β-actin (housekeeping gene) and the unmodified control using the $\Delta\Delta C_T$ method. Results are expressed as average +/- standard deviation. Statistical analysis was carried out using ANOVA (Tukey Model), p=0.05.

Immunocytochemistry

At the appropriate time points samples were removed from culture, washed with PBS and fixed with 4% paraformaldehyde/2% sucrose solution. Samples were stained for von Kossa using the previously described methods and prepared for immunocytochemical analysis of osteocalcin (10µg/ml R&D Systems) /actin (Oregon Green Phalloidin, 5µg/ml, Invitrogen UK) or CBFA1 (5µg/ml R&D Systems)/actin using the following methods. Following fixation samples were washed and permeabilised with a 0.05% Triton x100 solution in PBS for 5 minutes at 4°C then incubated with the primary antibody, diluted in 1%BSA: PBS, overnight at 4°C. Samples were then washed with a 0.1% Tween 20 (ICN Biomedicals) followed by incubation with Rhodamine conjugated goat IgG fraction to mouse IgG (Invitrogen) 1µg/ml in 1%BSA:PBS for osteocalcin and for CBFA1 primary antibodies a Texas Red goat anti-rat secondary, 1µg/ml in 1%BSA:PBS (Invitrogen) was used. Samples were incubated with the secondary antibodies for 1 hour at 37°C, followed by washing with the Tween 20 solution and incubation with Oregon Green Phalloidin, diluted in PBS, for 30 minutes at 4°C. Samples were washed then mounted onto microscope slides using Vectashield plus DAPI (Vector, UK) and visualised using confocal microscopy, Zeiss LSM510.

Results

Water Contact Angle data (figure 1) proved that addition of the –NH₂ presenting silanes to the glass substrates (figure 1A) affected the hydrophilic/hydrophobic properties of the base substrates. When CL3, CL4 and CL11 chain lengths were added to glass substrates, the resultant surfaces were more hydrophobic, as shown by an increase in contact angle (figure 1A). Regardless of the increase the WCA for all test substrates was below 90°, therefore still classed as hydrophilic. Substrates modified with CL4 showed a significantly

increased WCA compared with control substrates, whilst substrates modified with CL11 were significantly greater than all other control and test substrates. In parallel qualitative evaluation of the surface deposition of the -NH_2 groups across the surface was visualised using Ninhydrin staining (figure 1B). The Evaluation of the Ninhydrin staining associated with CL11 -NH_2 modifications (Figure 1B) proved that CL11 modifications resulted in a dense homogenous positive staining, reflecting the homogenous formation of an -NH_2 enriched surface, whilst staining associated with the CL3 and CL4 substrates was less dense and heterogeneous across the surface. Images are presented at a magnification that allows qualitative evaluation of the entire test substrate.

Further investigations into the enrichment of the surface with the -NH_2 groups was provided via XPS analysis (figure 2, table 1). With XPS data (table 1), culmination of the surface chemistry analysis proves that all chain lengths tested initially enriched the surface with -NH_2 groups. XPS was used to confirm silanization of the glass coverslips.

Representative wide energy survey scans and high resolution C 1s spectra of the control (unmodified glass), short chain modified (chain length 3) and long chain modified (chain length 11) are shown in Figure 2 with the corresponding quantitative data given in Table 1.

The control glass surface had peaks associated with carbon, silicone and oxygen, with C1s peak relating to adventitious carbon. Silanization of the coverslips was confirmed with the appearance of the N 1s peak at 400 eV. Table 1 shows that the short chain silane (CL3) has a higher N:C ratio(0.16-CL4, 0.0033-CL11)as expected as there is less carbon present. Curve fitting of the C1s spectra (Figure x d and f) for the CL3 and CL11 samples show components at C-C/C-H (285.0 eV) at C-O/C-N (286.5 eV), C=O/O=C-O (288.0 eV).

AFM analysis of the resulting -NH_2 silane layers proved that varying the chain length associated with the -NH_2 presenting silanes resulted in changes in the nanotopographical profiles (figure 3), most significantly with CL11 (LN). Representative AFM micrographs and associated analysis of control (unmodified glass), short chain modified (chain length 3) and long chain modified (chain length 11) are shown in Figure 3. Correlation of both qualitative (Figure 3A-C) and quantitative results (Figure 3D-F) clearly shows that the topographical profiles of the substrates changed after aminosilane modification. The roughness of clean glass (unmodified control) in $1.4\mu \times 1.4\mu$ area was 0.464 ± 0.001 nm; after short chain (CL4) aminosilane modifications, the roughness value reduced to 0.358 ± 0.001 nm; and after long chain (CL11) aminosilane modifications, it increased to 0.646 ± 0.008 nm. To analyse the uniformity/homogenous distribution of the nano features across the modified surface, the roughness of scan size from $100\text{nm} \times 100\text{nm}$ to $1.4\mu \times 1.4\mu$ from centre to outside was measured. The result in Figure 3D showed that although long chain aminosilane modified surface was rougher, it had a consistent roughness; for short chain aminosilane modified surface and the clean glass, the roughness changed over larger areas, demonstrating a heterogeneous nanotopographical profile. To further quantify the nanotopographical profile of the surfaces, line profiles at 3 distinct areas were evaluated. The line profiles showed that the peaks (nano-peaks) in LN (CL11) modified surface are taller, closer and overlap with each other, indicative of a homogenous/uniform distribution of nano-features; but the peaks in SN (CL3) modified surface are wider and do not overlap, again demonstrating a heterogeneous element to the nanotopographical profile associated with the SN (CL3) surface. The mean peak heights were 1.32nm for SN (CL3) modified surface and 5.66nm for LN (CL11) modified surface. All these results demonstrated that LN modified surface was

much more uniform with consistent structure in sub-micron scale, compare to SN modified surface. These findings were validated across a number of points across the test substrates.

Further tests were carried out to assess the adsorption properties, relevant to the production of osteoinductive substrates (figures 4 and 5). Qualitative analysis, von Kossa staining and visualisation of calcium deposition are represented by positive brown/black staining (figure 4), demonstrated that only surfaces modified with CL11 $-NH_2$ resulted in positive staining and therefore presence of a calcium rich layer on the surface. CL11 modifications produced a dense calcium rich matrix when cultured in contact with all tested concentrations of PBS, demonstrating a unique ability to absorb calcium from the local environment. This finding was further investigated and quantified using X-Ray Analysis (figure 5). At concentrations greater than 25% PBS only CL11 modifications demonstrated the absorption of phosphate ions from the local environment. This was confirmed statistically and directly reflected the positive pattern of von Kossa staining associated with only the CL11 modified substrates.

The differential adsorption profiles demonstrated by the change in chain length associated with the $-NH_2$ silane surfaces were reflected by protein adsorption profiles (figure 6).

Changing the chain length resulted in a change in the adsorption of fibronectin onto the surface, in both in the presence and absence of cells. Representative confocal images (figure 6A-B) demonstrate the difference in qualitative adhesion profiles associated with shorter chain (CL3, figure 6A) and CL11 modified substrates (figure 6B). When cultured in contact with shorter chain and control substrates fibronectin deposition was represented as a cohesive layer (represented by positive staining across the entirety of the surface), with notable pores in the adsorbed substrate. When cultured in contact with CL11 modified

substrates fibronectin adsorption gave a more roughened profile as shown in Figure 6B.

Analysis of the AFM data associated with fibronectin adsorption directly onto the modified surfaces confirmed that the profile associated with the adsorbed fibronectin layer was a direct comparison to the surfaces prior to adsorption. Generally height profiles (figure 6C and D) associated with the CL3 -NH₂ modified glass increased slightly, but were maintained below 1nm. Fibronectin coated CL11 resulted in an increase in the height profiles associated with the nanopеaks on the CL11 surface, these were roughly doubled in magnitude to approximately 1-1.5nm, but the periodicity and distinctiveness of the nanopеaks associated with the surface were maintained (figure 6E and 6F) and the increased roughness associated with the CL11 surface was visually observed in figure 6B.

Changes in initial protein adsorption had a direct correlation to material induced osteogenic differentiation, when cultured in contact with MSC in basal conditions. Well characterised adult hMSCs were cultured in direct contact with all -NH₂ modified substrates in basal medium for time periods up to 28 days in the absence of exogenous biological factors. The osteogenic potential of the surfaces was determined via profiling the mRNA expression of collagen I, CBFA1, osteopontin, osteonectin, osteocalcin and sclerostin via real time PCR (figure 7). For analysis by real time PCR the entire adherent cell population was lysed, therefore results are representative of the entire adherent cell population and were normalised to the adherent cell number (via a house keeping gene β -actin) and the expression profile of the cells in unstimulated conditions i.e. the control. Therefore up-regulations are any value above one and are representative as an up-regulation on a single cell basis that is directly associated with the activity of all cells that are adhered to the modified test substrates. In addition to quantitative evaluation of mRNA profiles the

homogenous expression of the osteogenic markers, CBFA1 (transcription factor) and osteocalcin (marker of functional osteoblast activity) using fluorescent immunohistochemistry are shown in figure 8. Samples were also stained with von Kossa at 14 and 28 days to qualitatively evaluate the production of a calcified extra cellular matrix (figure 9).

Quantitative evaluation of the PCR results demonstrated a significant up regulation of the early transcription factor CBFA1 at days 14 and 28 (Figure 7A) for CL4 modifications, but not for CL11. In contrast significant increases in the up-regulation of osteopontin, osteonectin and osteocalcin (usually found downstream of CBFA1 expression) (Figure 7B-D) were consistently associated with CL11 modifications. Further evidence of the osteogenic potential of the CL11 modifications was demonstrated by the up-regulation of sclerostin (Figure 7E) at day 28, a marker of the mature osteocyte phenotype (a cell type with matrix remodelling capabilities). Further evidence of the highly osteoinductive nature of the CL11 modified surfaces was observed at the protein level by immunohistochemistry.

All $-NH_2$ modified materials (figure 8) supported hMSC adhesion throughout the 28 day test period and were positive for CBFA1 and osteocalcin at various time points. Only hMSC cultured in contact with CL11 modified $-NH_2$ substrates demonstrated an enhanced and homogenous expression of osteogenic markers across the entirety of the test substrate. By day 14 there was clear evidence of a well-defined osteocalcin rich matrix on CL11 modified substrates, and clear evidence of organisation of the matrix to form pits within the matrix, in alignment with the natural organisation of a matrix rich in osteogenic factors. By day 28 there was clear evidence of organisation of the matrix associated only with CL11 modifications (figure 8). These results suggest that there was up-regulation of osteogenic

markers associated with the introduction of $-NH_2$ groups, as proven by the weak expression of osteocalcin on CL3, CL4, substrates. Only MSC cultured in contact with CL11 modified substrates demonstrated a sustained and enhanced production of a matrix rich in osteogenic factors across the entirety of the surface, which was positive for von Kossa staining (figure 9). In addition there was clear evidence of reorganisation of the matrix between days 14 and 28 on the CL11 surfaces, which was further supported by significantly enhanced expression of sclerostin (a marker of a mature osteoblast phenotype) at the mRNA level (figure 7). All of the results proved that only CL11 modifications can induce an efficient and homogenous level of osteoinduction of MSC in basal conditions and this in turn is associated with a controlled homogenous distribution of sub-micron material properties, that is only associated with the use of CL11 $-NH_2$ modifications.

Discussion

Silane modifications have previously been proven to be a suitable approach to enrich a surface with a chemical group of interest, that can subsequently provide a level of control over cellular responses^(17, 23, 25, 26). To date the results from these experiments have been variable, this is due to a lack of knowledge concerning the different parameters i.e. chain length associated with specific silane chemistry, and the resulting properties of the silane monolayer which is presented to the cells i.e. thorough investigation of the resultant material properties at the sub-micron scale. This research determined the effect of chain length on the properties of an $-NH_2$ presenting silane monolayer at the sub-micron level and the osteoinductive effect of this on an adherent stem cell population. It was experimentally evidenced that controlling the chain length of a silane chemistry resulted in significant changes to the homogenous deposition of the $-NH_2$ group in the resultant silane

modified layer and associated nanotopographical profile, which can be exploited to enhance the previously osteoinductive effects of -NH_2 enriched surfaces.

Generally the WCA results were in line with previously published finding regarding expected measurements associated with -NH_2 monolayers (figure 1) ⁽²⁷⁻³⁰⁾. The difference in contact angle is a contribution of two factors: the exposed chemical groups on the surface and the surface roughness associated with the different chain lengths used to produce the resultant modified surface. The exact mechanism regarding the individual contributions of chain length, reaction time and temperature of aminosilane used and their effect on the hydrophobicity (contact angle) is beyond the scope of this study. In relation to this study and for the purpose of testing the resultant silane layers as osteoinductive surfaces the WCA results presented in this paper showed that all CL3, CL4 and CL11 surfaces are less hydrophilic than unmodified ones, which are in line with previously published findings .

The major difference in terms of chain lengths tested was associated with the stability and topographical profile of the silane monolayer, associated only with the CL11 modified surfaces. Surfaces modified with CL11 -NH_2 resulted in a homogenous deposition of the -NH_2 group across the entirety of the surface (figure 1 B Ninhydrin analysis) and the formation of distinct nanopeaks, which showed an element of order/organisation which was lacking with other chain lengths tested (figure 3). Similar results were previously observed by Yang et al. ⁽³¹⁾ and Tillman et al. ⁽³²⁾. These studies reported stronger hydrophobic effects among the longer carbon chain (CL11) compared with the shorter carbon chain (CL3). Yang demonstrated that for the longer carbon chain silanes, the monolayer formed by Langmuir-type kinetics experienced a transition from lying-down to standing-up geometries, resulting in a more homogenous deposition. A key feature of the modified surfaces used in this study was that

the modification should produce a homogenous substrate across the entirety of the surface, to ensure a homogenous cell response. This is an essential criterion in the development of any material that is designed to evoke a specific biological response in a spatially defined area. Again only CL11 $-NH_2$ modified surfaces met this criteria, as shown by homogenous positive Ninhydrin staining (figure 1) and AFM analysis (figure 3). Shorter chain silanes did not meet these design criteria as they had a heterogeneous distribution of $-NH_2$ deposition across the surface (figure 1 and 3). The heterogeneous nature of a silane layer, has previously been reported⁽³³⁾. The report detailed a “clumping” phenomena associated with shorted chain length silanes, a factor that could affect the stability of the coatings and their ability to withstand the in vitro environment and the vigorous washing associated with the Ninhydrin assay. The culmination of these findings was visualised in figure 1B that demonstrated large areas of no positive staining across the substrates, therefore presenting an inherent variability in the cell culture results that was directly associated with the heterogeneous deposition of the $-NH_2$ coatings on the surface that was associated with the CL3 and CL4 substrates. This design/stability criterion was not an issue for the CL11 modified substrates which consistently produced data that is indicative of a homogenous distribution of sub-micron material features across the entirety of the surface.

Previously periodicity of features on a chemically defined surface has been reported to be integral in the maintenance of the MSC phenotype^(2, 4, 34). In addition to providing a more stable and homogenous coating the CL11 chain length also provided a topographical profile that consisted of organised nano peaks which resulted in an ordered nano-roughness, a feature that was not as prevalent on other chain lengths tested (Figure 3). This topographical profile was maintained when proteins were absorbed onto the surface (Figure

6). The combination of the sharpened nanopikes/nanoroughness and homogenous distribution of the -NH_2 group across the surface, resulted in a surface that had favourable surface chemistry and topographical features, resulting in a highly osteoinductive surface. This combination of features was not observed with any other chain length and has not previously been reported in the literature. This data demonstrated that subtle changes in surface features, i.e. nano-roughness compared to periodicity of a nanotopographical profile can be exploited at the material design stage to control stem cell attachment and subsequent differentiation.

A key feature of osteoinductive/bone contacting materials is their ability to produce or support a calcified matrix; mineralization is an essential step in the regeneration of bone and material bone apposition. The ability of a substrate to self-mineralise, via selected adsorption of elements from the surrounding environment is a significantly beneficial material property in the development of biomimetic surfaces. The role of surface modification, specifically -NH_2 and -COOH modified layers, in enhancing the ability of a material to produce an apatite-like layer when submerged in stimulated body fluids has previously been reported⁽³⁵⁻³⁸⁾. Yet the role of varying the chain length with a view to optimising this process has not previously been reported. Previous studies have utilised CL3 and CL11 -NH_2 presenting silanes and compared these chemistries directly with other enriched surfaces i.e. -COOH and -CH_3 and found that -NH_2 presenting surfaces have a superior ability to absorb apatite like layers directly onto the surface. Within this research the superior ability of the CL11 -NH_2 modified surfaces to support the nucleation of selected minerals on the surface as a tool for inducing enhanced osteointegration was determined, using von Kossa staining for calcification (figure 4) and x-ray analysis to determine the ability

of the surface to adsorb phosphorous (figure 5). The focus of this study was not to fully characterise the resultant Ca/P layer on the different substrates, but to investigate the adsorption profiles as a potential mechanism that can be exploited in the osteoinductive properties of the -NH_2 modified substrates. Previously certain SAMs have been reported to support nucleation on surfaces⁽³⁹⁾ and within this study only CL11 modified -NH_2 substrates proved to have the ability to adsorb Phosphorus from the local environment and form a calcified matrix, both in the presence and absence of MSC. This enhanced adsorption profile was also associated with a change in fibronectin adhesion and associated only with the CL11 modified substrates (figure 6).

CL11 modified substrates resulted in a controlled deposition of dense roughened fibronectin matrices, both in proteinaceous and cell containing environments, a major contributing factor to enhanced levels of hMSC adhesion and induced osteogenesis^(6, 7, 14) (figures 7 -9). The relationship between preferential fibronectin adsorption onto an -NH_2 modified surface and potential osteoinduction of hMSCs has previously been reported, but the data obtained with this research directly compared different chain lengths of -NH_2 silanes and evidenced a direct correlation between the formation of a dense cohesive fibronectin matrix across the entirety of the test substrate and the resultant dense osteogenic matrix formed by the stem cells that become embedded in the mineralised/fibronectin rich matrix associated only with the CL11 modified surfaces, a factor that has not previously been reported. Within this study it was found that the direct adsorption of the fibronectin onto the CL11 modified surface increased the surface roughness of the test substrates, at the nano-scale, providing further osteoinductive stimulus, a factor that was again lacking in the other chain lengths tested.

We have previously reported on the potential of -NH_2 surface enrichment to induce levels of osteogenic expression of MSCs in vitro, but results associated with the previous research did not reflect a homogenous or sustained level of material induced osteoinduction across the entirety of the surface ⁽¹⁷⁾. Within this study it has been proven that only hMSCs cultured with CL11 modified substrates demonstrated a sustained and enhanced level of all osteogenic markers, apart from CBFA a transcription factor at the mRNA level. The lack of CBFA1 expression could be attributed to the fact that CBFA1 is an early up-regulator of the osteoinductive pathway associated with osteogenesis ⁽⁴⁰⁻⁴²⁾. Early up-regulation of CBFA1 often results in the up regulation of osteocalcin, a phenomena that was observed within the PCR studies associated with the CL11 substrates. Therefore the 7 day time point associated with the PCR studies within this paper may have been too late to detect early up-regulations of CBFA1 transcription factor. Despite this culmination of the PCR data provides evidence that supports the enhanced osteoinductive properties associated with the CL11 modification. At this point it is as important to note that other -NH_2 presenting chain lengths did not present a sustained up-regulation of osteogenic markers at either the mRNA (figure 7) or protein level (Figure 8). Therefore supporting the argument that the use of silane chemistry requires enhanced investigation/optimisation if the potential of material induced cell responses is to be improved upon. In addition only CL11 modified surfaces demonstrated homogenous osteocalcin expression across the entirety of the surface, providing qualitative evidence of structured matrices and matrix organisation. This was further supported by the expression of sclerostin, a marker of a mature osteoblast phenotype with remodelling capabilities. This combination of sustained up-regulation of osteogenic markers was not observed on any other modified substrate and was indicative of a mature osteogenic matrix. This was further substantiated by von Kossa staining (calcified

extra cellular matrix), for which hMSCs on CL11 substrates showed a positive dense calcified extra-cellular matrix deposition by day 7, resulting in a highly organised calcified osteogenic rich matrix by day 28 (figure 9). Qualitative evaluation of the matrix showed evidence of reorganisation and the formation of a “pit like “structure within the matrix by day 28. The enclosure of osteoblasts within calcified pits within the matrix is considered to be an indicative marker of osteocyte development ⁽⁴³⁾ and the production of mature bone tissue, this phenomena was only associated with the CL11 modifications. The enhanced level of osteogenic cell maturity and production of an organised osteogenic rich extra cellular matrix was only observed on the CL11 modified surfaces. It is essential to reiterate that the observed cellular response on the CL11 surfaces was homogenous across the entirety of the surface, therefore proving that modification with CL11 –NH₂ silanes is an effective mechanism to produce cost effective osteoinductive coatings on different base substrates over a large surface area ⁽⁴⁴⁾.

In summary the results from this research demonstrated that only the surface properties of coating stability, nanotopography, distribution of –NH₂ groups and associated hydrophilic properties, using CL11 modifications induced enhanced osteoinduction, and the production of phenotypic osteogenic matrix in vitro in the absence of exogenous biological stimuli. This is the first comprehensive study that has worked through varying the properties of a selected range of silane presenting –NH₂ chemistries with the aim of inducing osteogenic differentiation in hMSCs. The data obtained has proven that varying the chain length of silanes is a valid tool for controlling the sub-micron properties of SAMs, and that these surfaces have an integral role in the control of protein and cell responses. This degree of material characterisation should be applied to every individual cell contacting application.

Parallel studies have proven that the CL11 substrates that were highly osteoinductive (ability to induce osteogenesis in MSCs) did not display significantly enhanced osteoconductive (ability to enhance the function of osteoblasts) behaviour in vitro. Instead the shorter chain silanes supported osteoblast clustering and resulted in an upregulation of osteoblast activity and production of calcified matrices⁽⁴⁴⁾. This proves that different combinations of sub-micron material stimuli are required to increase the efficiency of different cell phenotypes in vitro.

This study has exploited this relationship to develop wherein synthetic chemical modification replaces the need for protein and peptide modifications, leading very excitingly to a cost effective, translatable and potentially scalable method and technology for coating substrates, for both in vitro and in vivo applications; that can potentially be applied to an array of clinically relevant base substrates due to the simplicity of the modification process. The translation of this optimised osteoinductive coating (CL11 –NH₂) onto PLGA substrates is described in the supplementary information and proves that his technology can be applied to an array of base substrates. The properties of the optimised silane layer provide enough stimuli to the biological environment to provide a homogenous osteoinductive stimulus to a stem cell population, and as such provide a basis for enhanced control of biological responses and plays an important role in future material design rationale.

Competing Interests

The data presented within this manuscript has been used to support the Patent – Osteoinductive Surfaces held by The University of Liverpool.

Authors Contributions

Sandra Fawcett carried out the cell culture, cell analysis and some material characterisation , Rui Chen carried out the advanced material characterisation and development a, Raechelle D'Sa carried out the XPS, Riaz Akhtar carried out post experimental analysis of the AFM data, Judith Curran carried out the immunofluorescence and confocal analysis. Judith Curran, Rui Chen and John Hunt conceived the study, designed the study, coordinated the study and drafted the manuscript. All authors gave final approval for publication.

Funding

This work was part funded by The Leverhulme Trust.

Figure Legends:

Figure 1: Surface characterisation of $-NH_2$ modified glass. Surface hydrophobicity was measured using static contact angle in water (A). 3 measurements were taken at random points across each surface (3 replicate readings per repeat). Surfaces became more hydrophobic with the addition of the $-NH_2$ silanes, but were still less than 90° . Contact angle results are shown as average \pm standard deviation, $n=4$ (3 replicates per repeat to ensure homogeneity across the substrates) and statistical analysis was carried out using one way ANOVA (Tukey model). Both CL4 and CL11 substrates were significantly higher than glass control substrates (denoted as * $p<0.01$); whilst CL11 was also significantly greater than CL3 and CL4 (denoted as # $p<0.01$). Deposition of the $-NH_2$ groups across the surfaces was visualised using Ninhydrin assays (B). Positive staining (purple) is representative of $-NH_2$ enriched areas. Positive staining was observed on CL3 and CL4 modified substrates, whilst CL11 substrates resulted in a positive expression of stain across the surface.

Figure 2: XPS spectra of silanized surfaces (a) WESS glass control (b) C1s glass control (c) WESS CL3 (d) C1s CL3 (e) WESS CL11 and (f) C1s CL11.

Figure 3: AFM analysis with scan size $1.4\mu \times 1.4\mu$. (A) Clean glass control; (B) Short chain, CL3, aminosilane modified glass; (C) Long chain, CL11, aminosilane modified glass.

Roughness measurements/profiles were generated at 3 locations across each test sample (3 measurements per repeat). (D) The roughness of clean glass, (CL3) and (CL11) modified surface vs the scan size for 100nm to 1400nm; (E) Line profiles for (CL3) modified surface; (F) Line profiles for (CL11) modified surface.

Figure 4: Modified samples were placed in contact with dH_2O (control), 25%, 50% and 100% PBS solutions and cultured for 24 hours at $37^\circ C$. Samples were stained using von Kossa techniques to visualise the presence of calcified deposits on the surface. Qualitative analysis shows that only CL11 modified surfaces resulted in the formation of a dense calcified matrix at all concentrations of PBS, $n=4$, images shown are representative of the whole data set.

Figure 5: The ability of the substrates to absorb phosphate ions directly onto the surface was quantified using elemental X-ray analysis (A) resulting in the formation of a Ca/P rich matrix on the surface. Only surfaces modified with CL11 $-NH_2$ demonstrated an ability to absorb phosphate ions onto the surface under all conditions tested. Statistical analysis was used to calculate the probability of phosphorous occurring on the surface based on the raw data (full details of the probability model are provided in the materials and method). 0=no probability and 1= high probability. 4 repeats were carried out and in each repeat points of analysis were generated at 5 distinct locations on the film, from these fields 10 spectra were generated at random.

Figure 6: Preferential protein adsorption was evaluated using 5 µg/ml solutions of fibronectin cultured in contact with the range of –NH₂ modified surfaces for 24 hours, stained using fluorescent immunohistochemistry and visualised using confocal (A and B) and topographical features were mapped using AFM (C and D). Adhesion profiles on CL4 (A) at 24 hours depicted porous matrix morphology, whilst fibronectin adsorption on CL11 (B) substrates resulted in a heterogeneous matrix, of fibronectin rich areas, forming a roughened wave like structure across the entirety of the substrate. Scale bars on confocal micrographs are 20 µm. The change in nano-roughness profiles associated with the adsorbed fibronectin onto the surfaces was characterised using AFM. Results from the AFM data demonstrates that when adsorbed onto –NH₂ modified surfaces, the resultant protein layer mirrored the underlying topographical features on the modified surface. This was particularly evident on CL11 (E and F) where individual nanopeaks could still be observed in the adsorbed protein layer. The presence of the protein layer did not alter the previously observed topographical profiles associated with the different CL –NH₂ substrates.

Figure 7: Real Time PCR analysis from human MSC cultured in contact with modified and control samples for 7, 14 and 28 days in basal culture medium. All samples were modified to the house keeping gene β-Actin and the unmodified control value using the standard $\Delta\Delta C_T$ equation. Samples were analysed for up-regulations of CBFA1 (A), osteopontin (B), osteonectin (C), osteocalcin (D) and sclerostin (E). Data is shown as mean +/- SD from n=4. Statistical analysis was carried out using ANOVA (Tukey model), p=0.05, statistical significance is shown by *.

Figure 8: Representative images of hMSC grown in contact with Control (unmodified glass) and –NH₂ modified glass (CL3, CL4 and CL11) for 14 and 28 days under basal conditions in

vitro and stained for osteogenic markers CBFA1 (transcription factor, positive staining is red in colour in the cell nuclei) and osteocalcin (major matrix component of osteogenic matrix, red in colour). Cells are also stained for cell nuclei (DAPI, blue) and cytoskeletal actin (green). All test substrates maintained viable cell adhesion throughout the test period. Only cells grown in contact with CL11 displayed a highly dense osteogenic positive extra cellular matrix and evidence of matrix organisation, resulting in the formation of a dense osteocalcin rich matrix on the surface.

Figure 9: hMSC grown in contact with $-NH_2$ modified glass (A-F) and unmodified control (G-H) in basal conditions and stained for von Kossa at 14 (A, C, E, G) and 28 days (B, D, F, H). Dense positive von Kossa staining is clearly evident with the CL11 modified materials at 14 days (E) with evidence of remodelling of the calcified matrix by day 28 (F). von Kossa staining was classed as negative on unmodified controls and CL3 and CL4 modifications throughout the test period.

Table 1: XPS characterisation: elemental composition of surfaces with/without silane modification. An $-NH_2$ surface that was not highly osteoinductive (CL3) was used in direct comparison with the highly osteoinductive CL11 $-NH_2$ modified surface to determine the effect of O/C, N/C and Si/C ratios within the silane monolayer associated with varying chain length. XPS derived at. % values for silane modified surfaces.

Supplementary Figures:

Supplementary Figure 1: Clean 12mm glass cover slips were coated with chromium using an Emtech 575x sputter coater (Emtech, UK), to provide a surface for the PLGA film to form hydrogen bonds with. 100 μ l of 10 % 85:15 PLGA (Sigma, UK) in chloroform (UOL chemical

stores, UK) was spin coated onto the chromium coated cover slips using a WS-400B-6NPP/LITE spin coater (Laurell Technologies Corporation, UK). Oxygen plasma was used to functionalize the polymer (Emtech, UK), at the previously optimised settings of 30kW for 2 minutes (optimisation data not included). Samples were then modified following the same silanisation protocol previously described for glass coverslips in the materials and methods section. Samples were characterised using WCA and qualitative evaluation using Ninhydrin (details in materials and methods). The PLGA films were hydrophilic due to the plasma treatment used prior to silanisation (figure 1A). The focus of this study was to characterise the effect of varying the chain length (CL) on the resultant properties of the $-NH_2$ enriched surface. Modification with $-NH_2$ silanes significantly reduced the WCA compared to the PLGA control, *. CL11 modifications were also associated with a further significant reduction in WCA compared to the CL3 and CL4 modifications **. The final value for CL11 was comparable to the CL11 values obtained on glass (figure 1).

Qualitative evaluation of positive Ninhydrin staining showed that the densest homogenous staining was observed on CL11, whilst there was also evidence of positive staining on CL4 modified PLGA. These findings were in agreement with the ability of CL11 $-NH_2$ silanes to form an enriched modified surface on glass and PLGA films, which resulted in a change in WCA and positive Ninhydrin staining. These results prove the transferable nature of the surface modification from glass to PLGA.

Supplementary Figure 2: Representative images of hMSC grown in contact with Control (unmodified PLGA) and $-NH_2$ modified PLGA (CL3, CL4 and CL11) for 14 and 28 days under basal conditions in vitro and stained for osteogenic markers CBFA1 (transcription factor, positive staining is red in colour in the cell nuclei) and osteocalcin (major matrix component

of osteogenic matrix, red in colour). Cells are also stained for cell nuclei (DAPI, blue) and cytoskeletal actin (green). All test substrates maintained viable cell adhesion throughout the test period. Only cells grown in contact with CL11 displayed a positive expression of CBFA1 (transcription factor) at day 14 associated with positive osteocalcin expression, which was representative of matrix formation. By day 28 cells grown in contact with the CL11 modified surfaces demonstrated a dense osteocalcin matrix, formation of a dense osteocalcin rich matrix was only observed on CL11 modified PLGA.

References

- [1] Cabezas MD, Eichelsdoerfer DJ, Brown KA, Mrksich M, Mirkin CA. Combinatorial screening of mesenchymal stem cell adhesion and differentiation using polymer pen lithography. *Methods Cell Biol* 2014; 119: 261-76.
- [2] Curran JM, Chen R, Stokes R, Irvine E, Graham D, Gubbins E, *et al.* Nanoscale definition of substrate materials to direct human adult stem cells towards tissue specific populations. *J Mater Sci Mater Med* 2010; 21: 1021-9.
- [3] Lapointe VL, Fernandes AT, Bell NC, Stellacci F, Stevens MM. Nanoscale Topography and Chemistry Affect Embryonic Stem Cell Self-Renewal and Early Differentiation. *Adv Healthc Mater* 2013.
- [4] McMurray RJ, Gadegaard N, Tsimbouri PM, Burgess KV, McNamara LE, Tare R, *et al.* Nanoscale surfaces for the long-term maintenance of mesenchymal stem cell phenotype and multipotency. *Nat Mater* 2011; 10: 637-44.
- [5] Amini AR, Laurencin CT, Nukavarapu SP. Bone tissue engineering: recent advances and challenges. *Crit Rev Biomed Eng* 2012; 40: 363-408.
- [6] Arima Y, Iwata H. Preferential adsorption of cell adhesive proteins from complex media on self-assembled monolayers and its effect on subsequent cell adhesion. *Acta Biomater* 2015; 26: 72-81.
- [7] Hao L, Fu X, Li T, Zhao N, Shi X, Cui F, *et al.* Surface chemistry from wettability and charge for the control of mesenchymal stem cell fate through self-assembled monolayers. *Colloids Surf B Biointerfaces* 2016; 148: 549-556.
- [8] Hao L, Li T, Yang F, Zhao N, Cui F, Shi X, *et al.* The correlation between osteopontin adsorption and cell adhesion to mixed self-assembled monolayers of varying charges and wettability. *Biomater Sci* 2017; 5: 800-807.
- [9] Benoit DS, Schwartz MP, Durney AR, Anseth KS. Small functional groups for controlled differentiation of hydrogel-encapsulated human mesenchymal stem cells. *Nat Mater* 2008; 7: 816-23.
- [10] Celiz AD, Smith JG, Patel AK, Hook AL, Rajamohan D, George VT, *et al.* Discovery of a Novel Polymer for Human Pluripotent Stem Cell Expansion and Multilineage Differentiation. *Adv Mater* 2015; 27: 4006-12.
- [11] Chen M, Zhang Y, Zhou Y, Zhang Y, Lang M, Ye Z, *et al.* Pendant small functional groups on poly(ϵ -caprolactone) substrate modulate adhesion, proliferation and differentiation of human mesenchymal stem cells. *Colloids Surf B Biointerfaces* 2015; 134: 322-331.
- [12] Dalby MJ, Gadegaard N, Oreffo RO. Harnessing nanotopography and integrin-matrix interactions to influence stem cell fate. *Nat Mater* 2014; 13: 558-69.

- [13] Engler AJ, Sen S, Sweeney HL, Discher DE. Matrix elasticity directs stem cell lineage specification. *Cell* 2006; 126: 677-89.
- [14] Wang M, Cheng X, Zhu W, Holmes B, Keidar M, Zhang LG. Design of biomimetic and bioactive cold plasma-modified nanostructured scaffolds for enhanced osteogenic differentiation of bone marrow-derived mesenchymal stem cells. *Tissue Eng Part A* 2014; 20: 1060-71.
- [15] Huang J, Grater SV, Corbellini F, Rinck S, Bock E, Kemkemer R, *et al.* Impact of order and disorder in RGD nanopatterns on cell adhesion. *Nano Lett* 2009; 9: 1111-6.
- [16] McNamara LE, McMurray RJ, Biggs MJ, Kantawong F, Oreffo RO, Dalby MJ. Nanotopographical control of stem cell differentiation. *J Tissue Eng* 2010; 2010: 120623.
- [17] Curran JM, Chen R, Hunt JA. Material induced mesenchymal stem cell differentiation. *Biomaterials* 2010; 31: 1463-4.
- [18] Lin M, Wang H, Ruan C, Xing J, Wang J, Li Y, *et al.* Adsorption force of fibronectin on various surface chemistries and its vital role in osteoblast adhesion. *Biomacromolecules* 2015; 16: 973-84.
- [19] Dobbenga S, Fratila-Apachitei LE, Zadpoor AA. Nanopattern-induced osteogenic differentiation of stem cells - A systematic review. *Acta Biomater* 2016; 46: 3-14.
- [20] Phillips JE, Petrie TA, Creighton FP, Garcia AJ. Human mesenchymal stem cell differentiation on self-assembled monolayers presenting different surface chemistries. *Acta Biomater* 2010; 6: 12-20.
- [21] Kilian KA, Bugarija B, Lahn BT, Mrksich M. Geometric cues for directing the differentiation of mesenchymal stem cells. *Proc Natl Acad Sci U S A* 2010; 107: 4872-7.
- [22] Mathieu PS, Lobo EG. Cytoskeletal and focal adhesion influences on mesenchymal stem cell shape, mechanical properties, and differentiation down osteogenic, adipogenic, and chondrogenic pathways. *Tissue Eng Part B Rev* 2012; 18: 436-44.
- [23] Curran JM, Pu F, Chen R, Hunt JA. The use of dynamic surface chemistries to control msc isolation and function. *Biomaterials* 2011; 32: 4753-60.
- [24] Curran JM, Tang Z, Hunt JA. PLGA doping of PCL affects the plastic potential of human mesenchymal stem cells, both in the presence and absence of biological stimuli. *J Biomed Mater Res A* 2009; 89: 1-12.
- [25] Kuddannaya S, Chuah YJ, Lee MH, Menon NV, Kang Y, Zhang Y. Surface chemical modification of poly(dimethylsiloxane) for the enhanced adhesion and proliferation of mesenchymal stem cells. *ACS Appl Mater Interfaces* 2013; 5: 9777-84.
- [26] Paredes V, Salvagni E, Rodriguez-Castellon E, Gil FJ, Manero JM. Study on the use of 3-aminopropyltriethoxysilane and 3-chloropropyltriethoxysilane to surface biochemical modification of a novel low elastic modulus Ti-Nb-Hf alloy. *J Biomed Mater Res B Appl Biomater* 2015; 103: 495-502.
- [27] Chauhan AK, Aswal DK, Koiry SP, Gupta SK, Yakhmi JV, Sürgers C, *et al.* Self-assembly of the 3-aminopropyltrimethoxysilane multilayers on Si and hysteretic current-voltage characteristics. *Applied Physics A* 2008; 90: 581-589.
- [28] Howarter JA, Youngblood JP. Optimization of silica silanization by 3-aminopropyltriethoxysilane. *Langmuir* 2006; 22: 11142-7.
- [29] Mansur HS, Orefice RL, Vasconcelos WL, Lobato ZP, Machado LJ. Biomaterial with chemically engineered surface for protein immobilization. *J Mater Sci Mater Med* 2005; 16: 333-40.
- [30] Terracciano M, Rea I, Politi J, De Stefano L. Optical characterization of aminosilane-modified silicon dioxide surface for biosensing. *Journal of the European Optical Society-Rapid publications* 2013; 8.
- [31] Yang Y, Bittner AM, Baldelli S, Kern K. Study of self-assembled triethoxysilane thin films made by casting neat reagents in ambient atmosphere. *Thin Solid Films* 2008; 516: 3948-3956.
- [32] Tillman N, Ulman A, Schildkraut JS, Penner TL. Incorporation of phenoxy groups in self-assembled monolayers of trichlorosilane derivatives. Effects on film thickness, wettability, and molecular orientation. *J Am Chem Soc* 1988; 110: 6136-44.
- [33] Schwartz DK. Mechanisms and kinetics of self-assembled monolayer formation. *Annu Rev Phys Chem* 2001; 52: 107-37.

- [34] Curran JM, Stokes R, Irvine E, Graham D, Amro NA, Sanedrin RG, *et al.* Introducing dip pen nanolithography as a tool for controlling stem cell behaviour: unlocking the potential of the next generation of smart materials in regenerative medicine. *Lab Chip* 2010; 10: 1662-70.
- [35] Tavafoghi M, Brodusch N, Gauvin R, Cerruti M. Hydroxyapatite formation on graphene oxide modified with amino acids: arginine versus glutamic acid. *J R Soc Interface* 2016; 13: 20150986.
- [36] Zheng Y, Xiong C, Zhang S, Li X, Zhang L. Bone-like apatite coating on functionalized poly(etheretherketone) surface via tailored silanization layers technique. *Mater Sci Eng C Mater Biol Appl* 2015; 55: 512-23.
- [37] Toworfe GK, Composto RJ, Shapiro IM, Ducheyne P. Nucleation and growth of calcium phosphate on amine-, carboxyl- and hydroxyl-silane self-assembled monolayers. *Biomaterials* 2006; 27: 631-42.
- [38] Shen J, Qi Y, Jin B, Wang X, Hu Y, Jiang Q. Control of hydroxyapatite coating by self-assembled monolayers on titanium and improvement of osteoblast adhesion. *J Biomed Mater Res B Appl Biomater* 2017; 105: 124-135.
- [39] Toworfe GK, Bhattacharyya S, Composto RJ, Adams CS, Shapiro IM, Ducheyne P. Effect of functional end groups of silane self-assembled monolayer surfaces on apatite formation, fibronectin adsorption and osteoblast cell function. *J Tissue Eng Regen Med* 2009; 3: 26-36.
- [40] Takeda S, Bonnamy JP, Owen MJ, Ducy P, Karsenty G. Continuous expression of Cbfa1 in nonhypertrophic chondrocytes uncovers its ability to induce hypertrophic chondrocyte differentiation and partially rescues Cbfa1-deficient mice. *Genes Dev* 2001; 15: 467-81.
- [41] Ducy P. Cbfa1: a molecular switch in osteoblast biology. *Dev Dyn* 2000; 219: 461-71.
- [42] Ducy P, Zhang R, Geoffroy V, Ridall AL, Karsenty G. *Osf2/Cbfa1*: a transcriptional activator of osteoblast differentiation. *Cell* 1997; 89: 747-54.
- [43] Blonder J, Xiao Z, Veenstra TD. Proteomic profiling of differentiating osteoblasts. *Expert Rev Proteomics* 2006; 3: 483-96.
- [44] Fawcett SA, Curran JM, Chen R, Rhodes NP, Murphy MF, Wilson P, *et al.* Defining the Properties of an Array of -NH₂-Modified Substrates for the Induction of a Mature Osteoblast/Osteocyte Phenotype from a Primary Human Osteoblast Population Using Controlled Nanotopography and Surface Chemistry. *Calcif Tissue Int* 2017; 100: 95-106.

Table 1: XPS derived at.% values for silane modified surfaces

	At. %			
	C 1s	N 1s	O 1s	Si 2p
Glass Control	20.9 \pm 3.14	0	52.1 \pm 2.6	27.0 \pm 0.9
CL4	58.4 \pm 0	8.5 \pm 0.6	19.7 \pm 0.2	13.4 \pm 0.3
CL11	62.6 \pm 0.3	2.1 \pm 0.8	21.8	13.5 \pm 0.3

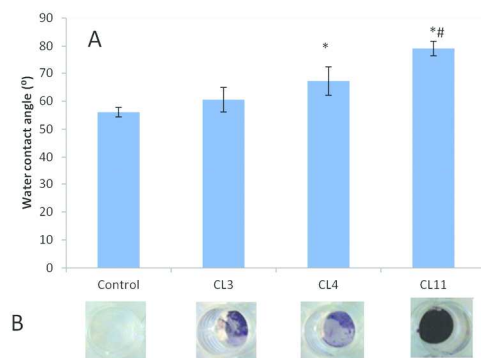


Figure 1

Figure 1: Surface characterisation of -NH_2 modified glass. Surface hydrophobicity was measured using static contact angle in water (A). 3 measurements were taken at random points across each surface (3 replicate readings per repeat). Surfaces became more hydrophobic with the addition of the -NH_2 silanes, but were still less than 90° . Contact angle results are shown as average \pm standard deviation, $n=4$ (3 replicates per repeat to ensure homogeneity across the substrates) and statistical analysis was carried out using one way ANOVA (Tukey model). Both CL4 and CL11 substrates were significantly higher than glass control substrates (denoted as * $p<0.01$); whilst CL11 was also significantly greater than CL3 and CL4 (denoted as # $p<0.01$). Deposition of the -NH_2 groups across the surfaces was visualised using Ninhydrin assays (B). Positive staining (purple) is representative of -NH_2 enriched areas. Positive staining was observed on CL3 and CL4 modified substrates, whilst CL11 substrates resulted in a positive expression of stain across the surface.

190x142mm (300 x 300 DPI)

Acc

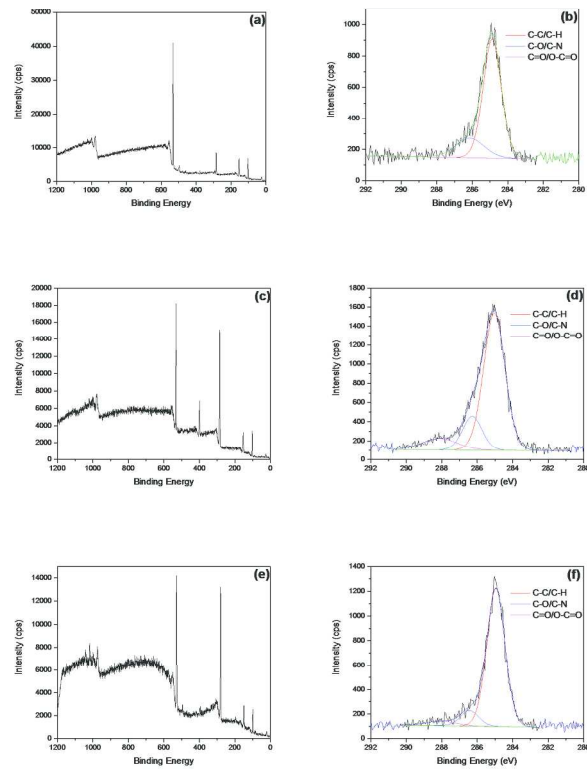


Figure 2

Figure 2: XPS spectra of silanized surfaces (a) WESS glass control (b) C1s glass control (c) WESS CL3 (d) C1s CL3 (e) WESS CL11 and (f) C1s CL11.

254x338mm (300 x 300 DPI)

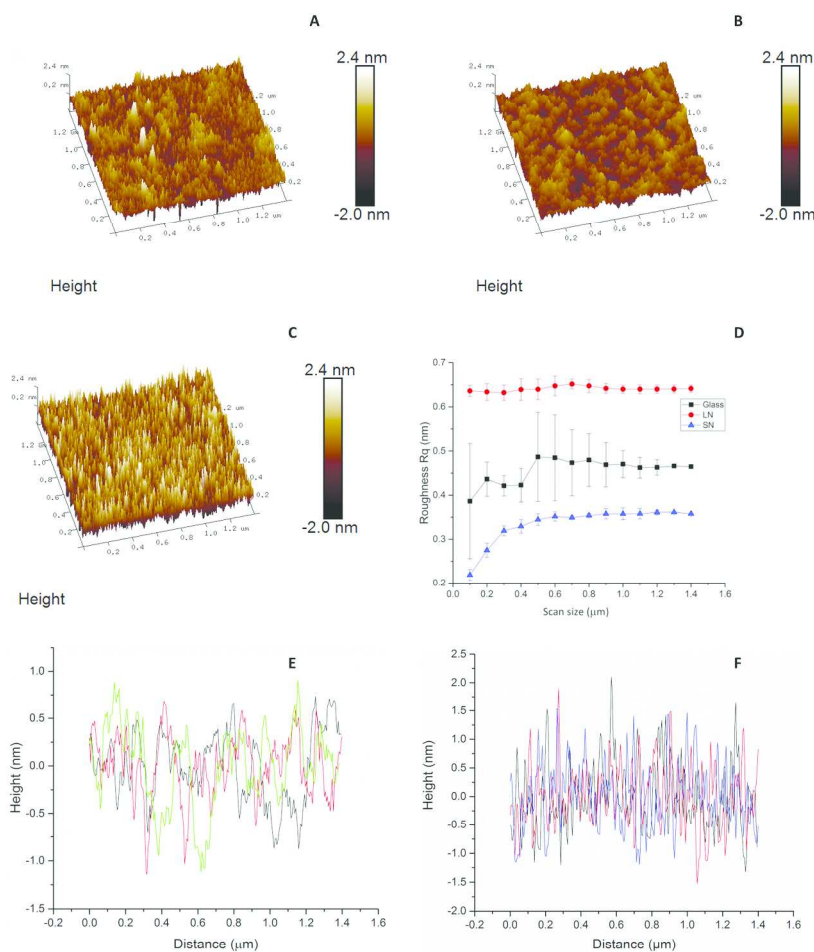


Figure 3

Figure 3: AFM analysis with scan size $1.4\mu \times 1.4\mu$. (A) Clean glass control; (B) Short chain, CL3, aminosilane modified glass; (C) Long chain, CL11, aminosilane modified glass. Roughness measurements/profiles were generated at 3 locations across each test sample (3 measurements per repeat). (D) The roughness of clean glass, (CL3) and (CL11) modified surface vs the scan size for 100nm to 1400nm; (E) Line profiles for (CL3) modified surface; (F) Line profiles for (CL11) modified surface.

275x397mm (300 x 300 DPI)

A

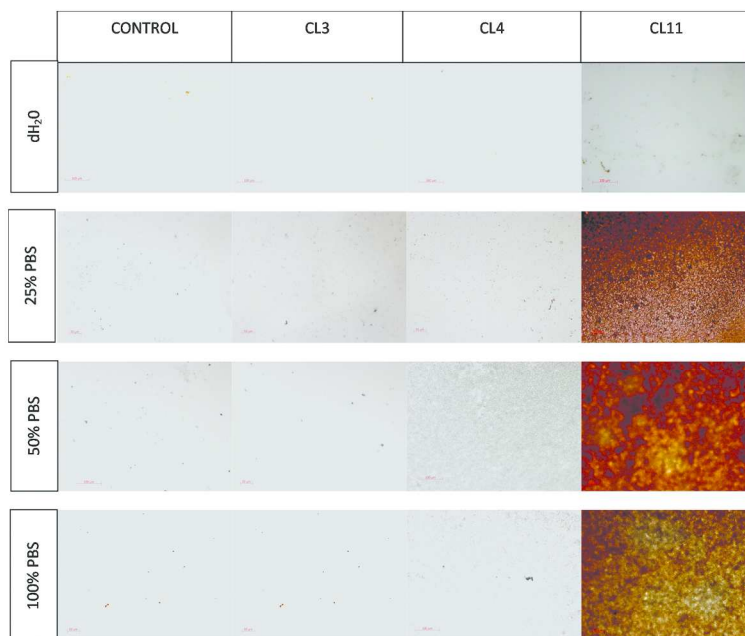
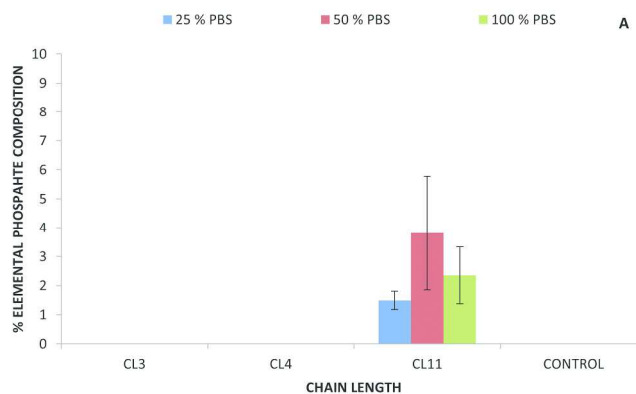


Figure 4

Modified samples were placed in contact with dH₂O (control), 25%, 50% and 100% PBS solutions and cultured for 24 hours at 37°C. Samples were stained using von Kossa techniques to visualise the presence of calcified deposits on the surface. Qualitative analysis shows that only CL11 modified surfaces resulted in the formation of a dense calcified matrix at all concentrations of PBS, n=4, images shown are representative of the whole data set.

190x275mm (300 x 300 DPI)

A



	Control	CL3	CL4	CL11
Water	0	0	0	0
25% PBS	0	0	0	0.43
50% PBS	0	0	0	1
100% PBS	0	0	0	0.9

Data derived from a probability model of phosphorous occurring on the surface. 0= no probability and 1= high probability.

Figure 5: The ability of the substrates to absorb phosphate ions directly onto the surface was quantified using elemental X-ray analysis (A) resulting in the formation of a Ca/P rich matrix on the surface. Only surfaces modified with CL11 -NH₂ demonstrated an ability to absorb phosphate ions onto the surface under all conditions tested. Statistical analysis was used to calculate the probability of phosphorous occurring on the surface based on the raw data (full details of the probability model are provided in the materials and method). 0=no probability and 1= high probability. 4 repeats were carried out and in each repeat points of analysis were generated at 5 distinct locations on the film, from these fields 10 spectra were generated at random.

275x397mm (300 x 300 DPI)

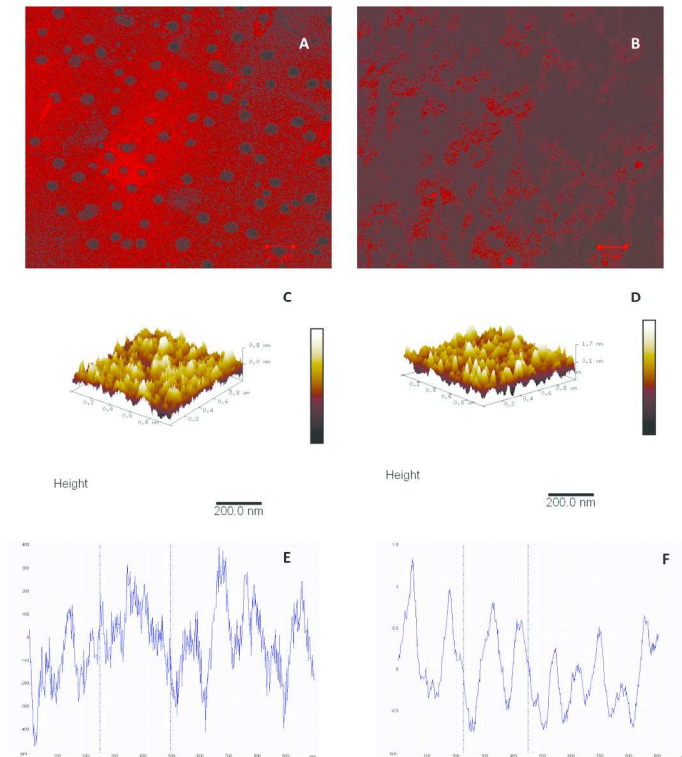


Figure 6

Figure 6: Preferential protein adsorption was evaluated using 5 μ g/ml solutions of fibronectin cultured in contact with the range of $-NH_2$ modified surfaces for 24 hours, stained using fluorescent immunohistochemistry and visualised using confocal (A and B) and topographical features were mapped using AFM (C and D). Adhesion profiles on CL4 (A) at 24 hours depicted porous matrix morphology, whilst fibronectin adsorption on CL11 (B) substrates resulted in a heterogeneous matrix, of fibronectin rich areas, forming a roughened wave like structure across the entirety of the substrate. Scale bars on confocal micrographs are 20 μ m. The change in nano-roughness profiles associated with the adsorbed fibronectin onto the surfaces was characterised using AFM. Results from the AFM data demonstrates that when adsorbed onto $-NH_2$ modified surfaces, the resultant protein layer mirrored the underlying topographical features on the modified surface. This was particularly evident on CL11 (E and F) where individual nano-peaks could still be observed in the adsorbed protein layer. The presence of the protein layer did not alter the previously observed topographical profiles associated with the different CL $-NH_2$ substrates.

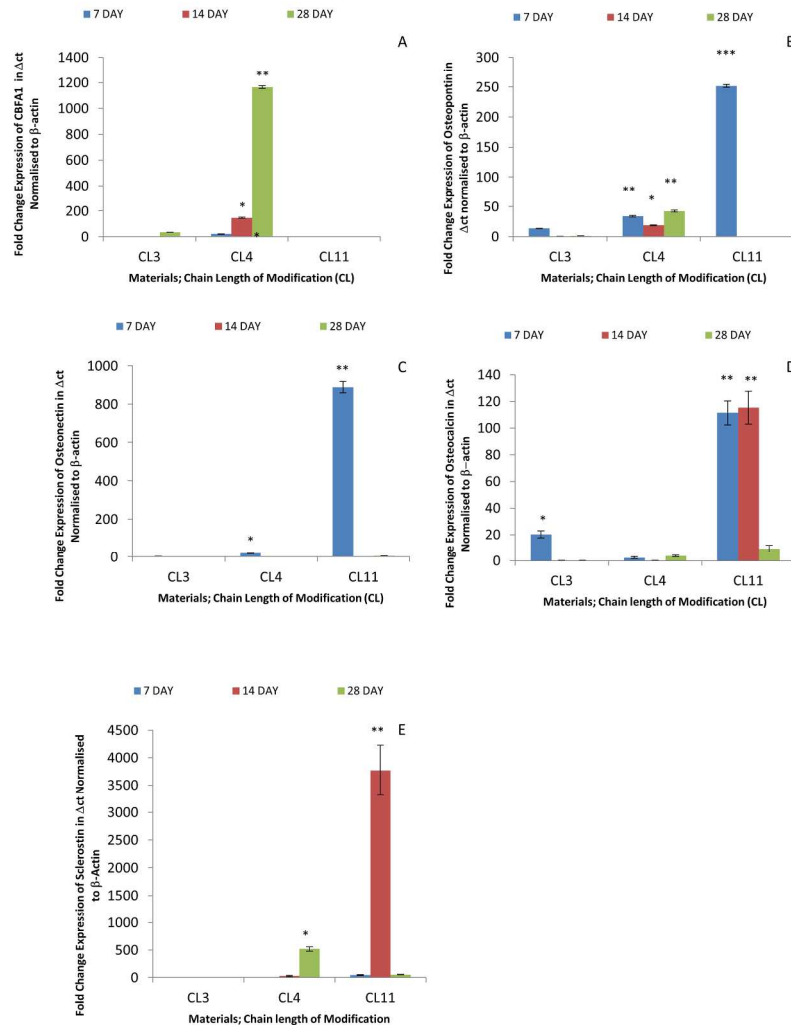


Figure 7

Real Time PCR analysis from human MSC cultured in contact with modified and control samples for 7, 14 and 28 days in basal culture medium. All samples were modified to the house keeping gene β -Actin and the unmodified control value using the standard $\Delta\Delta_{CT}$ equation. Samples were analysed for up-regulations of CBFA1 (A), osteopontin (B), osteonectin (C), osteocalcin (D) and sclerostin (E). Data is shown as mean \pm SD from $n=4$. Statistical analysis was carried out using ANOVA (Tukey model), $p=0.05$, statistical significance is shown by *.

275x397mm (300 x 300 DPI)

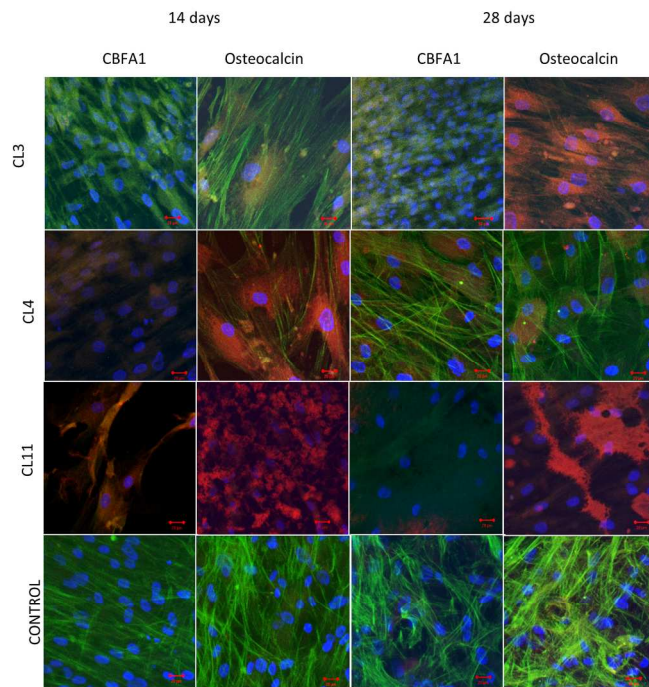


Figure 8

190x275mm (300 x 300 DPI)

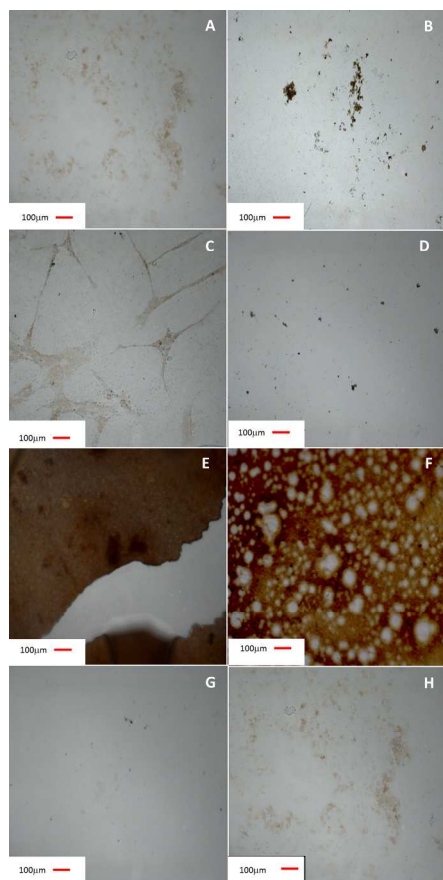


Figure 9

Figure 9: hMSC grown in contact with $-NH_2$ modified glass (A-F) and unmodified control (G-H) in basal conditions and stained for von Kossa at 14 (A, C, E, G) and 28 days (B, D, F, H). Dense positive von Kossa staining is clearly evident with the CL11 modified materials at 14 days (E) with evidence of remodeling of the calcified matrix by day 28 (F). von Kossa staining was classed as negative on unmodified controls and CL3 and CL4 modifications throughout the test period.

190x275mm (300 x 300 DPI)

A